Featured in Physics

Optimal Cooling of Multiple Levitated Particles through Far-Field Wavefront Shaping

Jakob Hüpfl,[1] Nicolas Bachelard,[1,2,*] Markus Kaczvinszki,[1] Michael Horodynski,[1] Matthias Kühmayer,[1] and Stefan Rotter[1,†]

[1]Institute for Theoretical Physics, Vienna University of Technology (TU Wien), A–1040 Vienna, Austria
[2]Université de Bordeaux, CNRS, LOMA, UMR 5798, F-33405 Talence, France

(Received 1 April 2021; revised 7 June 2022; accepted 17 January 2023; published 22 February 2023)

Light forces can be harnessed to levitate mesoscopic objects and cool them down toward their motional quantum ground state. Roadblocks on the way to scale up levitation from a single to multiple particles in close proximity are the requirements to constantly monitor the particles' positions as well as to engineer light fields that react fast and appropriately to their movements. Here, we present an approach that solves both problems at once. By exploiting the information stored in a time-dependent scattering matrix, we introduce a formalism enabling the identification of spatially modulated wavefronts, which simultaneously cool down multiple objects of arbitrary shapes. An experimental implementation is suggested based on stroboscopic scattering-matrix measurements and time-adaptive injections of modulated light fields.

DOI: 10.1103/PhysRevLett.130.083203

Exploiting light for the manipulation of matter has led to remarkable achievements like optical tweezers [1,2] or Bose-Einstein condensates [3]. A recent and exciting endeavor lies in using laser light to cool mesoscopic objects down to their motional quantum ground state [4]. To decouple these objects from their environment and make them directly accessible through micromanipulation, one laser levitates them in vacuum [5]. While promising remarkable opportunities for sensing [6–8], or for testing quantum physics [9,10], levitation so far strongly relies on local information. Take, as an example, tweezer-assisted cavity-cooling schemes that were recently applied to reach the ground state of a nanometer-size bead [11] through an approach known as coherent scattering [12–14]. There, performances are constrained by the ability to position the object within the optical mode [15–17]. In feedback-cooling schemes [18], the position of a particle is constantly monitored to bring the system to its ground state [19,20]. Yet, the process of monitoring is structurally subject to imprecisions [21] that limit the cooling efficiency. Moreover, despite recent advances in the cooling and manipulation of two levitated particles [22–26], current cooling schemes are hard to multiplex to a large number of particles. Alongside the difficulty to form multiple traps in close proximity due to optical binding [27], these limitations make levitation difficult to scale up to many coupled particles or from being applied simultaneously to rotational and translational degrees of freedom.

Yet, even when light from the control laser gets scattered by one or multiple levitated objects, it carries information about the objects' geometry and motion toward the far field. The bookkeeping of this information is conveniently organized in the scattering matrix, connecting the spatial profiles (i.e., wavefronts) of incoming and outgoing fields. Routinely measured even for complex systems [28–30], the scattering matrix has already provided access to tailor-made fields for applications in bioimaging [31–34] or quantum optics [35,36].

In this Letter, we demonstrate a novel procedure to distill from the scattered field the wavefronts necessary to manipulate several levitated objects in parallel. This approach can cool down or heat up multiple particles of nontrivial shapes experiencing complex motion. Notably, our cooling scheme applies to multiple coupled optomechanical resonators realized by nano-objects trapped in a standing wave. Capable of handling different motional degrees of freedom simultaneously, our procedure is also remarkably robust against reduced access to scattered-field information as necessary to be implemented in state-of-the-art setups.

Our starting point is the scattering matrix $\boldsymbol{S}$, which relates any incoming wave on a medium $|\Psi_{\text{in}}\rangle$ to the outgoing field scattered toward the far field, $|\Psi_{\text{out}}\rangle = \boldsymbol{S}|\Psi_{\text{in}}\rangle$ [Fig. 1(a)]. To get access to the observable of interest, $\boldsymbol{S}$ must be recast into a linear operator representing this observable. Take as an example a static scattering system, where the information on the time involved in the scattering process is represented by the time-delay (TD) operator $\boldsymbol{Q}_{\text{TD}} = -i\boldsymbol{S}^{\dagger}\partial_{\omega}\boldsymbol{S}$ [37,38]. Featuring a derivative with respect to the light's frequency ω, this Hermitian operator $\boldsymbol{Q}_{\text{TD}}$ contains the time each of its eigenstates spends inside the system as a corresponding real eigenvalue. To cool down moving particles, however, the observable of interest is not the time delay, but the shift in the particles' total energy. Moreover, rather than being static, the system we consider here follows a dynamic yet slow evolution—i.e., on a timescale larger than the light field's time delay. As shown in an accompanying article [39], the linear scattering operator that provides access to this energy

shift (ES) turns out to be a different operator $\boldsymbol{Q}_{\mathrm{ES}}(t) = -i\boldsymbol{S}^{\dagger}(t)\partial_t\boldsymbol{S}(t)$ involving a time derivative ∂_t of the instantaneous scattering matrix $\boldsymbol{S}(t)$ that is dynamically changing due to the particles' motion and measured at time t. A variant of this operator was introduced by Avron *et al.* in the context of mesoscopic electron transport [40] to describe how driven charge pumps pass electrons through a conductor [41]. Here, we study the reverse situation: Rather than operating a fermionic charge pump by a temporal change of the system, we inject a suitably shaped bosonic field to induce an optomechanical modification of the system itself. Importantly, injecting eigenstates of $\boldsymbol{Q}_{\mathrm{ES}}(t)$ changes a collective property of the system (its total energy) rather than just the motion of individual constituents [42].

At any given time, $\boldsymbol{Q}_{\mathrm{ES}}$ can be harnessed to identify wavefronts generating optical forces instantaneously reducing the total energy of a multiparticle system. Figure 1(a) displays a setup composed of a multimode waveguide filled with nano-objects of arbitrary shapes experiencing random motions. Two spatial light modulators (SLMs) located on both sides serve to constantly measure the instantaneous scattering matrix $\boldsymbol{S}(t)$ and inject spatially modulated wavefronts $|\Psi_{\mathrm{in}}(t)\rangle$. In the waveguide, any individual object of mass m and speed $\vec{v}_n$ executes an underdamped motion fulfilling

$$m\frac{d\vec{v}_n(t)}{dt} = \vec{F}_n(t) - m\gamma\vec{v}_n(t) + m\vec{g} + \vec{\xi}(t), \qquad (1)$$

in which $\vec{F}_n$ stands for the force produced by $|\Psi_{\mathrm{in}}\rangle$, γ the environmental friction, $\vec{g}$ gravity, and $\vec{\xi}(t)$ a white-noise process describing the coupling to the surrounding thermal bath. When the power of nonconservative forces (e.g., friction) remains smaller than the variations in the system's total energy E_{tot}, we demonstrate in Ref. [39] that an incoming field $|\Psi_{\mathrm{in}}\rangle$ produces optical forces that shift the total energy of the multiparticle system by an amount quantified by the energy-shift operator

$$\langle\Psi_{\mathrm{in}}|Q_{\mathrm{ES}}(t)|\Psi_{\mathrm{in}}\rangle = \frac{4\pi c}{\lambda}d_t E_{\mathrm{tot}}(t), \qquad (2)$$

where λ stands for the optical wavelength, c for the speed of light, and $d_t E_{\mathrm{tot}}$ for the instantaneous change in mechanical energy due to $|\Psi_{\mathrm{in}}\rangle$. From Eq. (2), we deduce that, at time t, the real eigenstate $|\Psi_{\mathrm{min}}(t)\rangle$ of the Hermitian operator

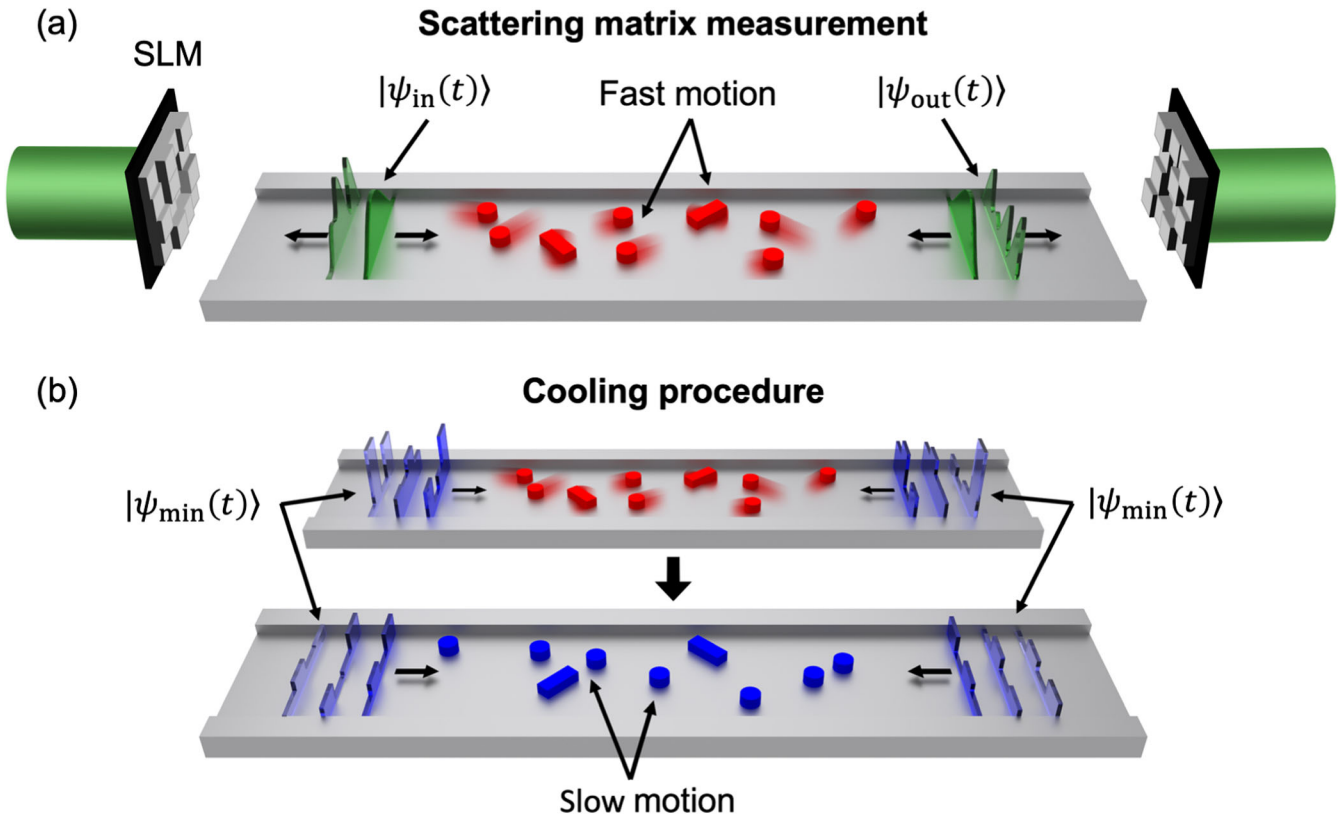

FIG. 1. (a) A multimode waveguide (gray) is filled with moving nano-objects with different shapes (bars and cylinders). SLMs are placed on both sides to inject modulated wavefronts $|\Psi_{\mathrm{in}}(t)\rangle$. The scattered-out wavefronts $|\Psi_{\mathrm{out}}(t)\rangle$ are recorded and serve to measure the instantaneous scattering matrix $\boldsymbol{S}(t)$ fulfilling $|\Psi_{\mathrm{out}}(t)\rangle = \boldsymbol{S}(t)|\Psi_{\mathrm{in}}(t)\rangle$. (b) Initially, the gas of nanoparticles follows a random motion, where objects rotate and/or translate (red objects). A succession of optimal cooling wavefronts $|\Psi_{\mathrm{min}}(t)\rangle$ gets injected from both sides (blue wavefronts) to optimally slow the particles' motion and cool down the gas (blue objects).

$Q_{\mathrm{ES}}(t)$ corresponding to its minimal (i.e., most negative) eigenvalue θ_{min} will perform an optimal reduction of the system's energy $[d_t E_{\mathrm{tot}}(t) = \theta_{\mathrm{min}}\lambda/4\pi c]$. We thus refer to $|\Psi_{\mathrm{min}}(t)\rangle$ as the optimal cooling state. For the same reason, optimal heating (i.e., increase of E_{tot}) is performed by the eigenstate of $Q_{\mathrm{ES}}(t)$ with the highest eigenvalue. Importantly, E_{tot} encompasses here both translational as well as rotational degrees of freedom, and the states $|\Psi_{\mathrm{min}}(t)\rangle$ are readily extracted from $Q_{\mathrm{ES}}(t)$. The operator $Q_{\mathrm{ES}}(t)$ itself is determined only through far-field measurements and comes without any prior knowledge of the particles' geometry or motion. Introduced here for a waveguide, Eq. (2) remains valid also for objects in free space that experience complex three-dimensional motion [43].

As illustrated in Fig. 1(b), for an underdamped gas of randomly moving objects (red particles), applying a succession of optimal cooling states ($|\Psi_{\mathrm{min}}(t)\rangle$) at sampled time steps effectively produces an artificial damping that cools down the ensemble (blue particles). In Fig. 2(a), we present results from the simulation of an ensemble of $N = 10$ silica beads (radius $r = 75$ nm, refractive index $n = 1.44$) that displays a low friction motion in the (x, z) plane fulfilling Eq. (1). The gas is initially thermalized, and its velocities follow a thermal distribution of mean

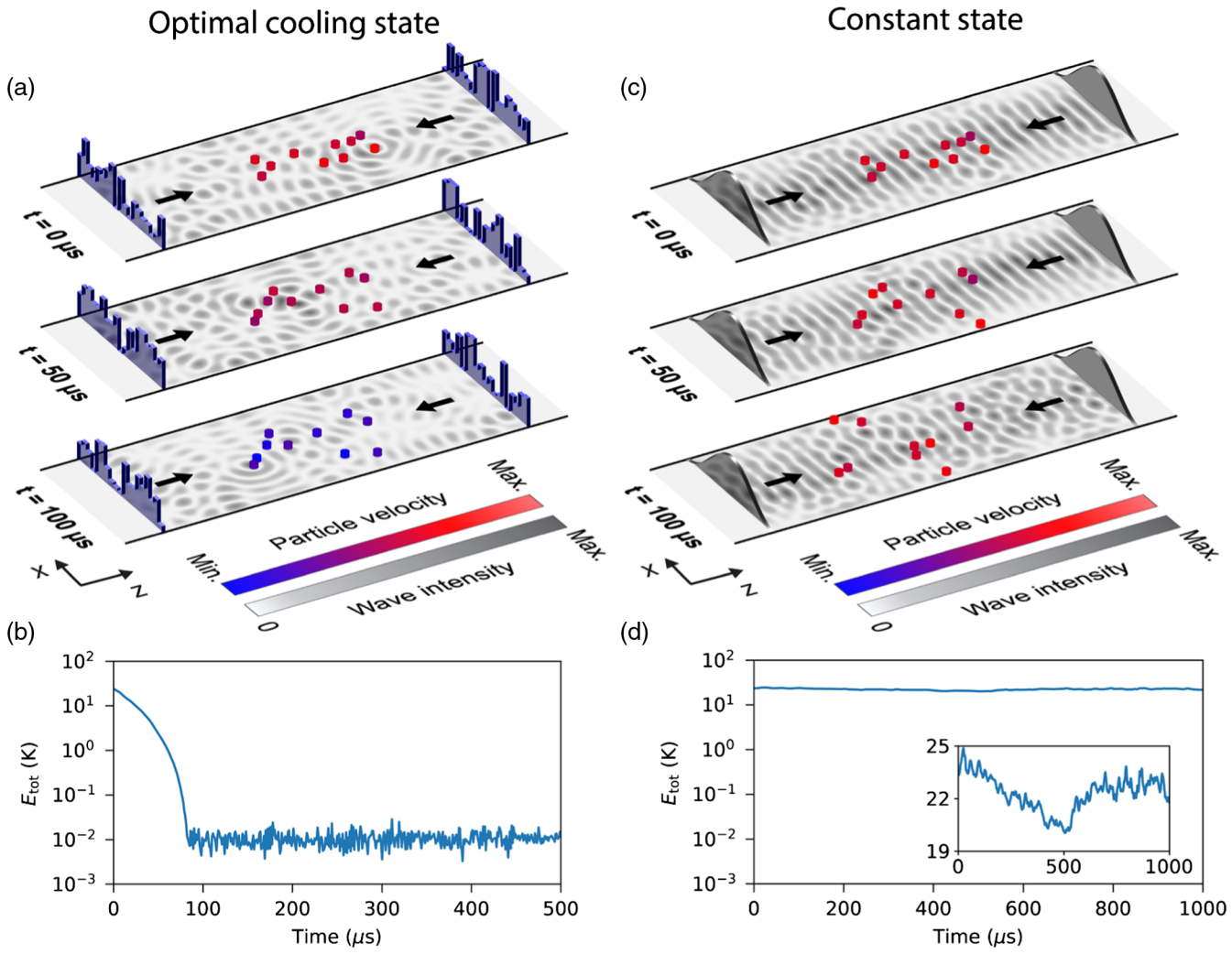

FIG. 2. (a) Confined in a waveguide with $M = 10$ transverse modes, a gas of $N = 10$ nanometer-size spherical particles ($r = 75$ nm, $m = 4.7 \times 10^{-18}$ kg, $\gamma = 6$ Hz) is initially in random motion (red beads in top panel, $t = 0$ μs). Over time, a succession of optimal cooling wavefronts (blue discontinuous lines on both leads) produces complex scattered fields in the waveguide (black and white intensity). At each time step, the $\boldsymbol{S}$ matrix corresponding to the particles' current locations is evaluated, $\boldsymbol{Q}_{\mathrm{ES}}(t)$ is computed, and its lowest eigenstate $|\Psi_{\mathrm{min}}(t)\rangle$ is applied to reduce E_{tot}. While optimal wavefronts are applied, the speeds of individual particles decrease progressively, as indicated by their colors in the three panels for times $t = 0$ μs (top), 50 μs (middle), and 100 μs (bottom), gradually transitioning from red to blue. (b) Log-scale evolution of E_{tot} during the procedure of (a). (c) For comparison, the gas shown in (a) is submitted to a constant incoming wavefront (waveguide's fundamental mode, gray curves in both leads). The particles wander around without cooling down. (d) Log-scale evolution of E_{tot} during the procedure of (c). The small fluctuations in energy are shown in the enlargement in the inset.

absolute value $\bar{v}_0 = 13\,\mathrm{mm/s}$ (temperature of $T_{\mathrm{env}} = 30\,\mathrm{K}$). Here, gravity in Eq. (1) is negligible and the total energy results solely from its kinetic contribution. The particles are confined within a multimode waveguide featuring $M = 10$ transverse modes, and they experience forces produced by a monochromatic field (wavelength $\lambda = 532$ nm). $\boldsymbol{S}(t)$ is measured at a sampling rate $\Delta t_{\mathrm{cool}} = 1$ μs and the energy-shift operator is approximated by $\boldsymbol{Q}_{\mathrm{ES}}(t) \approx -iS^{\dagger}(t)[S(t) - S(t - \Delta t_{\mathrm{cool}})]/\Delta t_{\mathrm{cool}}$. The initial configuration of the particles is shown in Fig. 2(a) at $t = 0$ μs, together with the optimal cooling state $|\Psi_{\mathrm{min}}(t = 0)\rangle$ extracted from $\boldsymbol{Q}_{\mathrm{ES}}(t = 0)$. This state gets injected with an optical power $P_{\mathrm{in}} = 20$ nW for $\Delta t_{\mathrm{cool}} = 1$ μs before the new optimal cooling state [corresponding to the new $\boldsymbol{Q}_{\mathrm{ES}}(t + \Delta t_{\mathrm{cool}})$] is computed and injected for the same duration. The process is then iteratively repeated every Δt_{cool} [see Fig. 2(a) for snapshots at $t = 50$ and 100 μs] with Fig. 2(b) displaying the time evolution E_{tot}. We observe that the energy continuously drops by more than 3 orders of magnitude in ≈100 μs, corroborating that successively applying optimal wavefronts acts as an "artificial" damping [44]. For comparison, Fig. 2(c) shows the anticipated action on the gas when an unmodulated wavefront (the fundamental transverse mode) gets injected into the waveguide with the same power. This field randomly transfers momentum to individual elements such that the energy remains almost unchanged for short timescales [Fig. 2(d)]. For longer timescales (i.e., comparable with the dissipation rate), the system heats up until a macroscopic thermal steady state is reached (not shown). In Ref. [39], we show that the cooling efficiency is limited by the sampling time (shorter Δt_{cool} provides a prompter response to the particles' movements). Moreover, the cooling performance is maximized for a specific optical power that optimally balances the particles' motion. Videos depicting the procedures described in Figs. 2(a) and 2(c) are provided in Supplemental Material [45] Videos M1 and M2, respectively.

The energy-shift operator can also serve to simultaneously cool coupled resonators made of multiple trapped nano-objects. In Fig. 3(a), a trapping field (green shape, $|\Psi_{\mathrm{trap}}\rangle$, $\lambda_{\mathrm{trap}} = 1550$ nm) gets injected from both sides in the waveguide's fundamental mode to form a standing wave, whose maxima correspond to potential wells (concentric contours). Confined within these wells, five nanobeads ($r = 75\,\mathrm{nm}$) form a chain of coupled optomechanical resonators. Along the longitudinal direction z, each oscillator is characterized by a power spectral density $|S_{zz}|$ displaying a main individual resonance close to 40 kHz, whose frequency varies slightly depending on the particles' location along the chain, while the coupling among particles manifests itself through the presence of harmonics [blue curve, Fig. 3(c)]. Using a second laser, we reproduce the iterative procedure illustrated in Figs. 2(a) and 2(b) and send a succession of optimal cooling states $|\Psi_{\mathrm{min}}(t)\rangle$ while the trapping field remains. The dynamics of individual

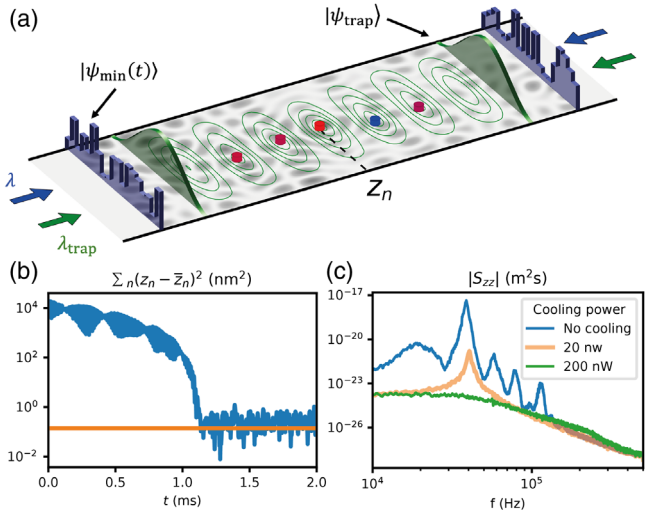

FIG. 3. (a) A trapping laser field (green waves, $|\Psi_{\mathrm{trap}}\rangle$) gets injected from both waveguide leads to form a standing wave (green concentric contours). Five nanobeads (positions $z_{n\in[1,5]}$) are confined at five maxima of the standing wave (mean positions $\bar{z}_{n\in[1,5]}$). A succession of optimal cooling states $|\Psi_{\mathrm{min}}(t)\rangle$ (blue wavefronts) is injected and reduces E_{tot}. (b) Log-scale time evolution of the variance of the particles' positions around their individual trapping locations (i.e., $\sum_n (z_n - \bar{z}_n)^2$) throughout the cooling procedure, using an optical power of 200 nW. The orange line corresponds to the energy level obtained through single-particle cold damping (scaled up by five particles) for an effective individual damping strength of $\gamma'_n \approx 320$ kHz. (c) Within its trap, each particle forms an optomechanical resonator. The blue curve displays the power spectral density $|S_{zz}|$ of the leftmost resonator at z_1 before cooling, while the orange and green curves correspond to cooling performed at 20 and 200 nW, respectively.

particles is described by Eq. (1), where a trapping-force contribution is added, while, according to Eq. (2), the cooling procedure reduces E_{tot} that now encompasses both the kinetic and potential energies of all the particles. As with conventional single-object cooling [18], by reducing the resonators' energy, our procedure pins the nano-objects at the bottom of their individual potentials. Using a power of 200 nW, Fig. 3(b) displays the time evolution of the combined fluctuations along z of all the particles around their respective trapping positions $\bar{z}_n$, which decrease by several orders of magnitude throughout the process. As expected, the procedure effectively increases motional damping and ultimately broadens individual resonances. Figure 3(c) displays in blue the power spectral density $|S_{zz}|$ of the leftmost particle along the chain before cooling. For the orange and green spectra, the system is cooled with 20 and 200 nW down to final states following thermal distributions with respective center-of-mass temperatures around 25 and 0.65 mK. Remarkably, when cooling is achieved, the coupling-induced harmonics disappear, while the quality factor of their main resonance reduces with cooling power until reaching a minimum for roughly 200 nW (similar behavior is observed for all nanobeads).

A video showing the cooling of the five particles in Fig. 3 is provided in Supplemental Material Video M3 [45].

Our scheme can be regarded as a many-body generalization of cold damping [21,44]. There, the speed v of a single trapped particle is monitored, which serves to exert a dampinglike force $F = -m\gamma' v$ of strength γ' that is opposed to the object's instantaneous motion. Schemes like cold damping are typically hard to transfer to multiple bodies in close proximity as the forces acting on each element become intertwined due to multiple scattering, making it difficult to monitor velocities. Here, the spatial degrees of freedom available through $\boldsymbol{S}$ serve to decipher these many-body motions and exert dampinglike forces on individual elements simultaneously [$F_n = -m_n\gamma'_n(t)v_n$ for the nth particle]. Nonetheless, compared to traditional cold damping, the individual damping strengths γ'_n evolve throughout the process as the routine seeks to reduce E_{tot} and applies larger (lower) damping to those elements with a faster (slower) movement. Ultimately, the system reaches a final state where the forces applied to every element correspond on average to a damping $\gamma'_n \approx 320$ kHz [orange line Fig. 3(b)]. This analogy with cold damping also emerges in the entropy pumping rate $-\dot{s}_{\mathrm{pu}}$, which, in feedback schemes, characterizes an extra entropy production originating from the action of the control loop [46,47]. Figure 4(a) shows that this entropy pumping rate progressively increases throughout the five-particle cooling of Fig. 3(b), before settling at a rate around 5 times the level expected for single-particle cold damping.

While our derivations implicitly rely on the assumption that $\boldsymbol{S}(t)$ is unitary (i.e., loss-free), this scheme is robust to missing information. For an $N = 10$-particle gas confined in an $M = 20$-mode waveguide, Fig. 4(b) shows the performance of the protocol introduced in Figs. 2(a) and 2(b) with $\boldsymbol{Q}_{\mathrm{ES}}(t)$ being assembled from an incomplete set of modes, (i.e., expressed within the basis of the first $M_P \leq 20$ modes), which emulates the impact of optical aberrations in the incoming field. The green dotted, orange dash-dotted, and blue dashed curves correspond to the temporal evolution of $E_{\mathrm{tot}}(t)$ obtained for $M_p = 8, 4$, and 2, respectively, while the black curve reports the cooling performed with the full set of modes (i.e., $M_p = M$). Reducing the available information degrades the cooling performance. When M_p decreases, the convergence time increases, while the efficiency worsens. Yet, we always observe significant cooling even when only a few modes are involved. Moreover, in the absence of a cavity, our cooling scheme is not only unaffected by laser phase noise, but we explain in Ref. [39] that it is also remarkably robust to measurement noise degrading the $\boldsymbol{S}$-matrix reconstruction. At last, we also stress that our procedure remains effective for nontrivial particle shapes. The Supplemental Material Video M4 [45] shows that an inhomogeneous mixture of differently shaped particles can also be cooled.

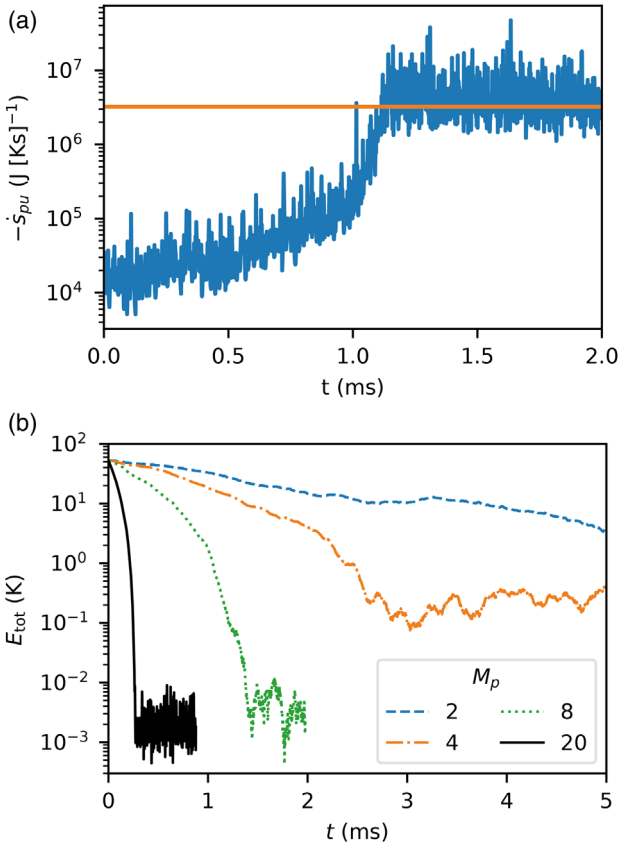

FIG. 4. (a) Log-scale time evolution of the entropy pumping rate $-\dot{s}_{\mathrm{pu}}$ throughout the cooling performed in Fig. 3(b). The orange line marks the level expected for single-particle cold damping performed with a strength of $\gamma' \approx 320$ kHz (scaled up by five particles). (b) Log-scale total energy evolution of an $N = 10$-particle gas (without trapping field) cooled using $M_p = 20$ (black solid), 8 (green dotted), 4 (orange dash-dotted), and 2 (blue dashed) modes among the waveguide's $M = 20$ modes, respectively.

The procedure can be implemented with current state-of-the-art modulator technology. As explained in Ref. [39], the maximum stroboscopic time span can be estimated by $\Delta t_{\mathrm{max}} \approx (\lambda/4)\sqrt{(\sum_{i=1} m_i/N_{\mathrm{d.o.f.}}k_B T_{\mathrm{env}})}$, in which $N_{\mathrm{d.o.f.}}$ stands for the total degrees of freedom. For the systems considered here, this time span lies around $\Delta t_{\mathrm{max}} \approx 10$ μs, which is within range of SLMs that already reach GHz frequencies [48].

In summary, we use scattered-field information to capture the collective motion of a complex system composed of mesoscopic objects. Assembled from the scattering matrix, a linear energy-shift operator enables the manipulation of multiple motional degrees of freedom to perform the cooling or heating of many-body systems. Implementable with current optical modulators, our approach is robust against information loss and noise while neither requiring particles' detection nor calibration. Using techniques such as online estimation [49] to identify efficient cooling states could result in a vast speedup of

our protocol. While currently classical, our model could be adapted to investigate the ground-state cooling of many-body systems, where quantum backaction becomes relevant. More generally, with its flexibility with respect to the particles' dimensions or shapes, our method could prove to be a crucial tool for quantum-state engineering in mesoscopic many-body systems [50], the realization of complex nanoheat engines [51], or for the assembly of dynamical materials [52,53].

We thank J. Bertolotti and Y. Louyer for helpful discussions and the team behind the open-source code NGSOLVE for assistance. Support by the Austrian Science Fund under Project No. P32300 (WAVELAND) and funding for N. B. from the European Union's Horizon 2020 research and innovation program under the Marie Skłodowska-Curie Grant Agreement No. 840745 (ONTOP) are gratefully acknowledged. The computational results presented were achieved using the Vienna Scientific Cluster.

J. H. and N. B. contributed equally to this work.

*Corresponding author.
nicolas.bachelard@gmail.com
†Corresponding author.
stefan.rotter@tuwien.ac.at

[1] A. Ashkin, J. M. Dziedzic, J. E. Bjorkholm, and S. Chu, Observation of a single-beam gradient force optical trap for dielectric particles, Opt. Lett. **11**, 288 (1986).
[2] W. D. Phillips and H. Metcalf, Laser Deceleration of an Atomic Beam, Phys. Rev. Lett. **48**, 596 (1982).
[3] M. H. Anderson, J. R. Ensher, M. R. Matthews, C. E. Wieman, and E. A. Cornell, Observation of Bose-Einstein condensation in a dilute atomic vapor, Science **269**, 198 (1995).
[4] J. Chan, T. P. M. Alegre, A. H. Safavi-Naeini, J. T. Hill, A. Krause, S. Gröblacher, M. Aspelmeyer, and O. Painter, Laser cooling of a nanomechanical oscillator into its quantum ground state, Nature (London) **478**, 89 (2011).
[5] A. Ashkin and J. M. Dziedzic, Feedback stabilization of optically levitated particles, Appl. Phys. Lett. **30**, 202 (1977).
[6] J. Chaste, A. Eichler, J. Moser, G. Ceballos, R. Rurali, and A. Bachtold, A nanomechanical mass sensor with yoctogram resolution, Nat. Nanotechnol. **7**, 301 (2012).
[7] G. Ranjit, D. P. Atherton, J. H. Stutz, M. Cunningham, and A. A. Geraci, Attonewton force detection using microspheres in a dual-beam optical trap in high vacuum, Phys. Rev. A **91**, 051805(R) (2015).
[8] G. Ranjit, M. Cunningham, K. Casey, and A. A. Geraci, Zeptonewton force sensing with nanospheres in an optical lattice, Phys. Rev. A **93**, 053801 (2016).
[9] O. Romero-Isart, A. C. Pflanzer, F. Blaser, R. Kaltenbaek, N. Kiesel, M. Aspelmeyer, and J. I. Cirac, Large Quantum Superpositions and Interference of Massive Nanometer-Sized Objects, Phys. Rev. Lett. **107**, 020405 (2011).
[10] D. Goldwater, M. Paternostro, and P. F. Barker, Testing wave-function-collapse models using parametric heating of a trapped nanosphere, Phys. Rev. A **94**, 010104(R) (2016).
[11] U. Delić, M. Reisenbauer, K. Dare, D. Grass, V. Vuletić, N. Kiesel, and M. Aspelmeyer, Cooling of a levitated nanoparticle to the motional quantum ground state, Science **367**, 892 (2020).
[12] U. Delić, M. Reisenbauer, D. Grass, N. Kiesel, V. Vuletić, and M. Aspelmeyer, Cavity Cooling of a Levitated Nanosphere by Coherent Scattering, Phys. Rev. Lett. **122**, 123602 (2019).
[13] S. Nimmrichter, K. Hammerer, P. Asenbaum, H. Ritsch, and M. Arndt, Master equation for the motion of a polarizable particle in a multimode cavity, New J. Phys. **12**, 083003 (2010).
[14] D. Windey, C. Gonzalez-Ballestero, P. Maurer, L. Novotny, O. Romero-Isart, and R. Reimann, Cavity-Based 3D Cooling of a Levitated Nanoparticle via Coherent Scattering, Phys. Rev. Lett. **122**, 123601 (2019).
[15] O. Romero-Isart, M. L. Juan, R. Quidant, and J. I. Cirac, Toward quantum superposition of living organisms, New J. Phys. **12**, 033015 (2010).
[16] D. E. Chang, C. A. Regal, S. B. Papp, D. J. Wilson, J. Ye, O. Painter, H. J. Kimble, and P. Zoller, Cavity opto-mechanics using an optically levitated nanosphere, Proc. Natl. Acad. Sci. U.S.A. **107**, 1005 (2010).
[17] P. F. Barker and M. N. Shneider, Cavity cooling of an optically trapped nanoparticle, Phys. Rev. A **81**, 023826 (2010).
[18] J. Gieseler, B. Deutsch, R. Quidant, and L. Novotny, Subkelvin Parametric Feedback Cooling of a Laser-Trapped Nanoparticle, Phys. Rev. Lett. **109**, 103603 (2012).
[19] F. Tebbenjohanns, M. L. Mattana, M. Rossi, M. Frimmer, and L. Novotny, Quantum control of a nanoparticle optically levitated in cryogenic free space, Nature (London) **595**, 378 (2021).
[20] L. Magrini, P. Rosenzweig, C. Bach, A. Deutschmann-Olek, S. G. Hofer, S. Hong, N. Kiesel, A. Kugi, and M. Aspelmeyer, Real-time optimal quantum control of mechanical motion at room temperature, Nature (London) **595**, 373 (2021).
[21] J. Millen, T. S. Monteiro, R. Pettit, and A. N. Vamivakas, Optomechanics with levitated particles, Rep. Prog. Phys. **83**, 026401 (2020).
[22] T. W. Penny, A. Pontin, and P. F. Barker, Sympathetic cooling and squeezing of two colevitated nanoparticles, Phys. Rev. Res. **5**, 013070 (2023).
[23] H. Rudolph, U. Delić, M. Aspelmeyer, K. Hornberger, and B. A. Stickler, Force-Gradient Sensing and Entanglement via Feedback Cooling of Interacting Nanoparticles, Phys. Rev. Lett. **129**, 193602 (2022).
[24] Y. Arita, G. D. Bruce, E. M. Wright, S. H. Simpson, P. Zemánek, and K. Dholakia, All-optical sub-kelvin sympathetic cooling of a levitated microsphere in vacuum, Optica **9**, 1000 (2022).
[25] J. Rieser, M. A. Ciampini, H. Rudolph, N. Kiesel, K. Hornberger, B. A. Stickler, M. Aspelmeyer, and U. Delić, Tunable light-induced dipole-dipole interaction between optically levitated nanoparticles, Science **377**, 987 (2022).

[26] J. Vijayan, Z. Zhang, J. Piotrowski, D. Windey, F. van der Laan, M. Frimmer, and L. Novotny, Scalable all-optical cold damping of levitated nanoparticles, Nat. Nanotechnol. **18**, 49 (2023).
[27] Y. Arita, E. M. Wright, and K. Dholakia, Optical binding of two cooled micro-gyroscopes levitated in vacuum, Optica **5**, 910 (2018).
[28] S. M. Popoff, G. Lerosey, R. Carminati, M. Fink, a. C. Boccara, and S. Gigan, Measuring the Transmission Matrix in Optics: An Approach to the Study and Control of Light Propagation in Disordered Media, Phys. Rev. Lett. **104**, 100601 (2010).
[29] S. Rotter and S. Gigan, Light fields in complex media: Mesoscopic scattering meets wave control, Rev. Mod. Phys. **89**, 015005 (2017).
[30] A. P. Mosk, A. Lagendijk, G. Lerosey, and M. Fink, Controlling waves in space and time for imaging and focusing in complex media, Nat. Photonics **6**, 283 (2012).
[31] *Wavefront Shaping for Biomedical Imaging*, edited by J. Kubby, S. Gigan, and M. Cui (Cambridge University Press, Cambridge, England, 2019).
[32] R. Horstmeyer, H. Ruan, and C. Yang, Guidestar-assisted wavefront-shaping methods for focusing light into biological tissue, Nat. Photonics **9**, 563 (2015).
[33] W. Lambert, L. A. Cobus, T. Frappart, M. Fink, and A. Aubry, Distortion matrix approach for ultrasound imaging of random scattering media, Proc. Natl. Acad. Sci. U.S.A. **117**, 14645 (2020).
[34] S. Jeong, Y.-R. Lee, W. Choi, S. Kang, J. H. Hong, J.-S. Park, Y.-S. Lim, H.-G. Park, and W. Choi, Focusing of light energy inside a scattering medium by controlling the time-gated multiple light scattering, Nat. Photonics **12**, 277 (2018).
[35] H. Defienne, M. Barbieri, I. A. Walmsley, B. J. Smith, and S. Gigan, Two-photon quantum walk in a multimode fiber, Sci. Adv. **2**, e1501054 (2016).
[36] D. Bouchet, S. Rotter, and A. P. Mosk, Maximum information states for coherent scattering measurements, Nat. Phys. **17**, 564 (2021).
[37] E. P. Wigner, Lower limit for the energy derivative of the scattering phase shift, Phys. Rev. **98**, 145 (1955).
[38] F. T. Smith, Lifetime matrix in collision theory, Phys. Rev. **118**, 349 (1960).
[39] J. Hüpfl, N. Bachelard, M. Kaczvinszki, M. Horodynski, M. Kühmayer, and S. Rotter, companion paper, Optimal cooling of multiple levitated particles: Theory of far-field wavefront shaping, Phys. Rev. A **107**, 023112 (2023).
[40] J. E. Avron, A. Elgart, G. M. Graf, and L. Sadun, Time-energy coherent states and adiabatic scattering, J. Math. Phys. (N.Y.) **43**, 3415 (2002).
[41] J. E. Avron, A. Elgart, G. M. Graf, and L. Sadun, Transport and dissipation in quantum pumps, J. Stat. Phys. **116**, 425 (2004).
[42] M. Horodynski, M. Kühmayer, A. Brandstötter, K. Pichler, Y. v. Fyodorov, U. Kuhl, and S. Rotter, Optimal wave fields for micromanipulation in complex scattering environments, Nat. Photonics **14**, 149 (2020).
[43] J. Schäfer, H. Rudolph, K. Hornberger, and B. A. Stickler, Cooling Nanorotors by Elliptic Coherent Scattering, Phys. Rev. Lett. **126**, 163603 (2021).
[44] F. Tebbenjohanns, M. Frimmer, A. Militaru, V. Jain, and L. Novotny, Cold Damping of an Optically Levitated Nanoparticle to Microkelvin Temperatures, Phys. Rev. Lett. **122**, 223601 (2019).
[45] See Supplemental Material at http://link.aps.org/supplemental/10.1103/PhysRevLett.130.083203 for movies depicting: 10 particles in a constant field (M1), the cooling process applied to 10 particles (M2), the cooling process applied to 5 trapped particles (M3), the cooling process applied to 10 particles with different shapes (M4).
[46] T. Munakata and M. L. Rosinberg, Entropy production and fluctuation theorems under feedback control: The molecular refrigerator model revisited, J. Stat. Mech. 05 (2012) P05010.
[47] T. Munakata and M. L. Rosinberg, Feedback cooling, measurement errors, and entropy production, J. Stat. Mech. 06 (2013) P06014.
[48] A. Smolyaninov, A. el Amili, F. Vallini, S. Pappert, and Y. Fainman, Programmable plasmonic phase modulation of free-space wavefronts at gigahertz rates, Nat. Photonics **13**, 431 (2019).
[49] L. Valzania and S. Gigan, Online learning of the transfer matrix of dynamic scattering media: Wavefront shaping meets multidimensional time series, arXiv:2210.04033.
[50] J. I. Cirac, M. Lewenstein, K. Mølmer, and P. Zoller, Quantum superposition states of Bose-Einstein condensates, Phys. Rev. A **57**, 1208 (1998).
[51] A. Dechant, N. Kiesel, and E. Lutz, All-Optical Nanomechanical Heat Engine, Phys. Rev. Lett. **114**, 183602 (2015).
[52] N. Bachelard, C. Ropp, M. Dubois, R. Zhao, Y. Wang, and X. Zhang, Emergence of an enslaved phononic bandgap in a non-equilibrium pseudo-crystal, Nat. Mater. **16**, 808 (2017).
[53] C. Ropp, N. Bachelard, D. Barth, Y. Wang, and X. Zhang, Dissipative self-organization in optical space, Nat. Photonics **12**, 739 (2018).